

Effects of Particle Size and Soil Bed on the Shear Strength of Materials in the Direct Shear Test

Thaveechai Kalasin^{1*}, Chayanan Khamchan², Auttawee Aoddej³

¹ Department of Civil Engineering, Faculty of Engineering, Rajamangala University of Technology Lanna, Chiang Mai, 50300, Thailand

² Thaitota Corporation LTD, Lamphun, 50100, Thailand

³ Chiangmai Springer Trading Limited Partnership, Chiang Mai, 50300, Thailand

* Corresponding author, e-mail: ithaasin@rmutl.ac.th

Received: 05 May 2022, Accepted: 25 October 2022, Published online: 15 November 2022

Abstract

Generally, direct shear apparatus is used to determine the shear strength parameters of soil and rock for designing a geotechnical engineering structure. However, the size of the shearing box and the soil sample is key for evaluating the shear strength parameters of test materials, and also testing conditions in the laboratory are different from site conditions. This research aimed to focus experimentally on the effect of particle size and the property of subgrade materials that were necessary keys for installing apparatuses for the direct shear test. According to the experimental results based on a 5 x 5 cm shear box, an increase in average particle size and coefficient of curvature could provide higher shear strength in terms of internal friction angle of the sample, but not for the case of higher value of the uniformity coefficient. Using both 5 x 5 cm and 30 x 30 cm shear boxes, a large B/D_{max} ratio is not the key for determining appropriate parameters when testing with samples that have a nearly uniform size. Samples varied in thickness of both the ballast and subgrade layers, were investigated and observed by a large shear box. It was found that good properties of subgrade materials affected the shear strength of ballast materials, and they provided underestimates of strength when the bottom of the shearing box was rigid. The modified parameter of ballast materials on the subgrade layer is suggested for obtaining strength parameters reflecting the ballasted track system.

Keywords

direct shear test, ballast materials, sand, railways, shear strength

1 Introduction

In the railway industry, the ballast material is a significant part of the railway ballast track, and it is valuable to have an optimal choice for low budget and low noise. The shear strength of ballast materials plays an important role, due to the movement of trains. However, it is degraded under the load-term service of train loading. Therefore, the behavior of ballast materials is a critical concern in railway design. In order to improve the engineering properties of ballast materials, many techniques have been proposed to satisfy the economic and engineering aspects [1–2]. The fouling of ballast materials is a key cause of track misalignment and poor levelling [3–4], and a clean and dense ballast layer is needed to replace the fouled ballast. In addition, a void contaminant index was suggested to be used, and the index was incorporated with void ratio, specific gravity, and gradation of both ballast and fouling materials [5–6].

Under-sleeper pads can reduce the settlement and the degradation of ballast materials, and this technique can provide larger contact areas between the ballast and the sleeper layers [2]. To obtain the shear strength of the ballast materials for designing the ballast track system, which transfers the vertical and horizontal loads to the ballast and subgrade layers, a direct shear test was determined to be an accurate and reasonable apparatus for testing this physical condition but, a change in the shear-box size was required to satisfy the particle size of the tested materials.

According to the findings from other research, the direct shear test can be grouped into three types. The first type is the standard test which is generally used to measure the shear strength of both cohesive and cohesiveless soils [7–10]. The second type is the in-situ test [11–13]. This method is good for testing under real conditions, but

the sample preparation and the shear plane are difficult to prepare for tested samples. The third type is a large direct shear box which is tested in the laboratory [1, 6, 14–22]. Although, this method can be used for testing large particle sizes, the effect of the box size and soil-bed properties cannot be considered. In order to develop the large shear test apparatus that reflects the site condition and the quality of the testing results, the summary of findings about the direct shear test are discussed here.

A large shear box was used to investigate the granular materials, and it was found that the high non-homogeneity deformation of a shear band provides stress-dilatancy. This was different from the experimental results of the small shear box [14]. Thus, there was a need to explore the effect of the box size and the condition of testing to the experimental condition. The width or diameter of the shear box, B depended on the maximum particle size, D_{\max} and the ratio of $B/D_{\max} = 10$ was mostly used for the direct shear test. In the case of a rock-filled dam, a coarse sample with a size particle smaller than 150 mm was tested by the size of the testing box was $15 \times 15 \times 15$ cm [7]. Box sizes $122.5 \times 122.5 \times 16$ cm, $63.2 \times 63.2 \times 16$ cm and $31.6 \times 31.6 \times 10$ cm were recommended for the coarse aggregate in the rock-filled dam, gravel, and sand materials, respectively [11, 14]. The testing results performed by the direct shear in the laboratory were equal to the results tested by the in-situ-direct shear test, but the nonlinear relationship of the shear and normal stress was apparent when using the in-situ test. Also, the sample preparation for direct shear testing in the laboratory might not reflect the same conditions as the on-site environmental conditions, so that in-situ-direct shear tests could be an alternative method to evaluate the shear strength parameters of rock-fill materials containing large particles. Thus, the cohesion parameter might be included if the Mohr-Coulomb's envelope was occupied to obtain the shear strength parameters. In practice, the cohesion parameter could be ignored for design procedures where the sample was rockfill materials [11]. A box sized $80 \times 80 \times 40$ cm was tested on a site of roller-compacted rockfill sandstone. The peak shear strength occurred when the horizontal displacement was about 4% of specimen length [12].

While the top box begins to shear, the gap between the top and bottom boxes becomes apparent and directly affects the direction of the shear force on the sample. If this gap progresses, the result of the shear force is inaccurate; therefore, the top box should be fixed for applying horizontal force [15–16]. The opening gap caused the

outflow of the sample during shearing and an inaccurate shear strength. However, the reasonable shear strength and shear behavior can be obtained when the gap is small [16]. If the shearing plane was not smooth, the lower shear strength could occur due to reducing contacted area, especially in the case of direct shear testing on the rock materials [17–18]. The pattern and direction of the rock bed affected the magnitude of the shear strength of the rock. In consequence, the maximum shear strength of the rock occurred when either the direction of shear testing was perpendicular to the direction of the rock bed [19, 23–26] or the increase of an angle between the bedding plane and the shear plane appeared [24–25].

The factors that affect the quality of testing results depended on the loading conditions, the shearing rate, the size of the shear box and the initial vertical stress on the samples [8–9]. The rate of shear loading for the direct shear test influences the magnitude of the shear strength. According to a numerical study, the effective rate is more than 0.02 m/s. If the shearing rate is high, the direction of the pushing load might not be on a horizontal axis [26]. The initial-vertical displacement will be a negative value, while the particle size is small, and the maximum horizontal shear force increases with decreasing layer height and initial void ratio [27].

Not only the specification of the direct shear apparatus affected on the magnitude of the shear strength of tested materials, but also the inhomogeneous property of tested samples contained with sand, gravel, or rock could provided the various results. So, the effect of composition of the tested sample was needed for determining the potential shear strength of the sample. The tested sample mixed with 30% rock mass, and tested with a minimum compression load of 37.2 kPa on the direct shear box, showed an increase of the internal friction angle and a decrease in cohesion [13]. Also, the vertical displacement was always positive during the test. However, the large particle size of the sample caused the direction of the lateral force to deviate from a pure horizontal axis. Thus, the lateral direction should be focused on during the test if highly accurate results are required [28].

The increase of angularity and sphericity indexes affected the shear strength of ballast samples [6, 20] in terms of internal friction angle and dilation [4, 21, 27]. However, the fine-material and water contents are the reasons for lower shear strengths and higher axial deformations of ballast materials. The maximum size of the ballast layer was 65 mm, and the thickness of the ballast layer was 30 cm.

However, the quality of ballast materials was degraded and broken to poor quality by supporting heavy and high traffic of train loadings. If the ballast material was crushed due to train loads, this possibly leads to poor quality of drainage materials, decreasing shear strength, reducing the internal friction angle, and increasing cohesion and dilatancy [22]. On the other hand, non-crushed ballast leads to unchanged porosity affecting the boundary and position of the shear band zone [29]. The particle size effect was investigated and suggested in the model test. It revealed that the variation in particle size affected the localization of maximum shear strain and, the boundary movement [10].

The effect of both the shear box size and the particle size on the shear strength parameters of the soil and rock samples is still unclear for describing the controlled parameters in terms of shear strength parameters. Thus, this research emphasized various effects of the B/D_{\max} ratio on Mohr-Coulomb's parameters. The main findings of this research can identify the suitable ratio of B/D_{\max} for the direct shear with changes in the average particle size, D_{50} . The main finding is also useful to select the B/D_{\max} ratio for the size of the shear box when the particle size of materials is larger than 4.75 mm. For most of the sample preparations used for direct shear testing, the sample was prepared in the shear box on a rigid plate. This might not be reflected in the properties of subgrade materials because the magnitude of shear strength parameters would be decreased with high settlement of the subgrade layer. This effect was not considered when the direct shear test was performed with the standard apparatus. Therefore, the properties of subgrade materials located at the lower layer of the ballast layer are investigated in order to observe the differential shear strength between the case of the ballast layer placed on the subgrade layer and the case of the ballast layer placed on the rigid base. The findings will be useful when the direct shear test is used to determine the designed parameters of ballast and subgrade materials.

2 Test equipment and scheme

2.1 Test equipment

To investigate the particle size effect, shear boxes sized 5×5 cm (the standard shear box) and 30×30 cm (the developed shear box) were used to test and investigate the effect of the B/D_{\max} ratio when the particle size is also varied but the type of soil is sand. The shear box consists of top and bottom parts, and the horizontal load was applied on the top shear box. While testing the sample, the horizontal and vertical loads were monitored and recorded by using the load

cells in horizontal and vertical directions. Also, the vertical and horizontal displacements were measured with a linear variable differential transformer (LVDT) at two positions located on the top and lateral shear boxes as shown in Fig. 1. This machine is developed for a 30×30 cm direct shear box. The 5×5 cm shear box was tested by the standard apparatus based on ASTM D 3080 [30]. In the case of subgrade properties affecting the shear strength parameters, the 30×30 cm shear box with two layers was used in this study, as shown in Fig. 1. The position of the shearing test was on the top. The top layer is the ballast layer, and the bottom layer was prepared and compared with the silty clay reflecting the site conditions.

2.2 Test scheme

2.2.1 Properties of ballast and sand samples

The density and particle size of sand, ballast and subgrade materials were investigated and tested. These properties were used for preparing samples for direct shear test. The density of each sample was equally controlled in each layer. The experiments of engineering properties were performed. The results of sand properties are shown in Fig. 2 and Table 1. The dry density of all sand samples was 13.6 kN/m^3 . All sand samples were poor grade, as determined by the coefficient of curvature ($C_c = 1-3$) and the uniformity coefficient ($C_u > 6$).

The granite-ballast materials were collected from the site of railway as shown in Fig. 4(a). The particle size of the crushed ballast materials was shown in Fig. 3. The maximum particle size of tested ballast was 30 mm based on the B/D_{\max} ratio (10:1) and the dry density of ballast materials in the field was 16 kN/m^3 .

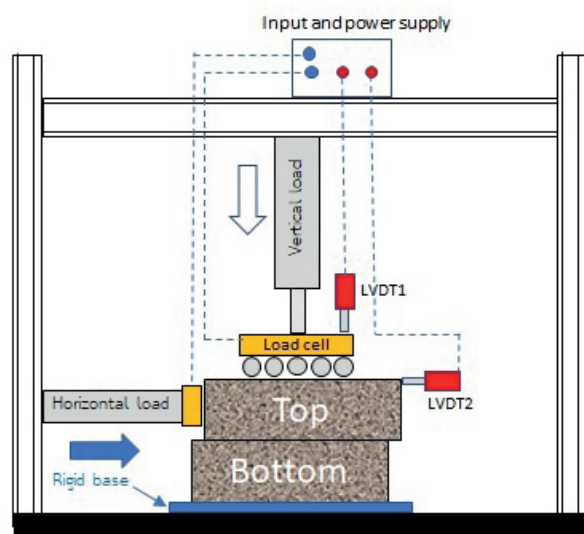


Fig. 1 Direct shear test with 30×30 -cm shear box

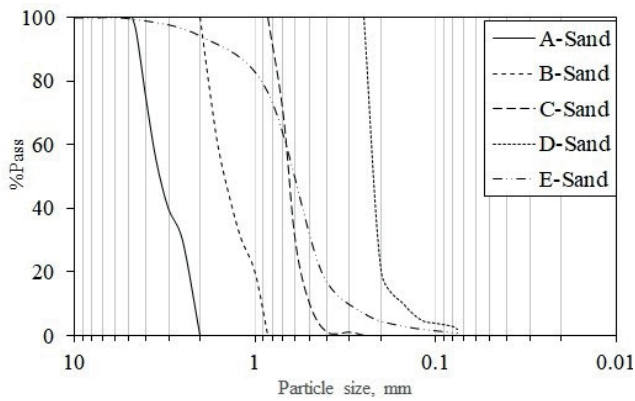


Fig. 2 Grain size distribution curves of tested sand

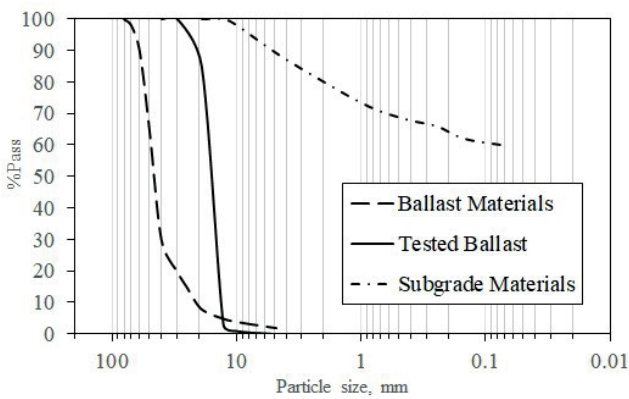


Fig. 3 Grain size distribution curves of ballast material, tested ballast materials and subgrade materials

Table 1 Particle size of sand samples tested by a box sized 5 × 5 cm

Group	D_{max} (mm)	D_{50} (mm)	C_u	C_c	Range of size (mm)	B/D_{max}
A-Sand	4.75	3.375	1.7	0.8	4.75-2	10.5:1
B-Sand	2.00	1.425	1.7	0.9	2-0.85	25:1
C-Sand	0.85	0.638	1.4	1.0	0.85-0.425	58.8:1
D-Sand	0.25	0.225	2.4	1.3	<0.25	200:1
E-Sand	4.75	0.600	2.3	1.1	<4.75	10.5:1

The subgrade material is inorganic silt of low to medium plasticity (CL) where more than 50% of materials are larger than 0.075 mm particle size, LL% = 33% and PI% = 17%. The total density of subgrade material was 14.6 kN/m³.

2.2.2 Sizes of shear boxes

In order to observe the effect of the particle size on the shear strength of sand, the various sizes of the sand sample were used for direct shear testing. The 5 × 5 cm shear box was used, and the preparation of samples could be classified into four groups, as shown in Table 1. The B/D_{max} ratio was greater than 10. The corrected area of both 5 × 5 cm and 30 × 30 cm shear boxes was considered to determine the shear strength of tested materials in this investigation.

2.2.3 Sample preparation of tested ballast and soil-bed

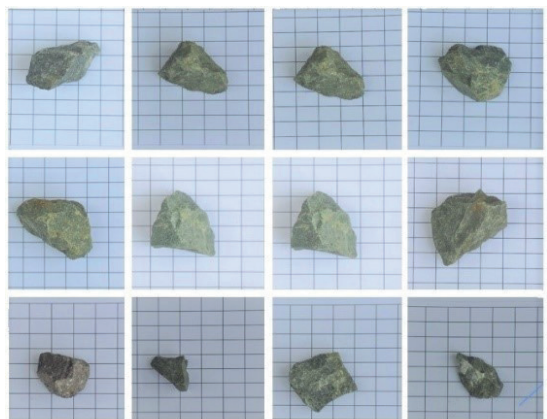
In order to investigate the effect of the soil bed under the ballast layer on the shear strength of ballast materials, the thickness of the ballast layer, H_b , and the thickness of the subgrade layer, H_s were varied. The maximum size of ballast materials collected from the field was 63 mm, however the size of the tested ballast was less than 30 mm for samples of the direct shear testing. The top layer was the tested-ballast layer. This layer was compacted into a dense state. The shape of the tested ballast, showed in Fig 4(b), was nearly similar to an icosahedron, with a sphericity index of 0.7. The ballast layer was prepared by controlling the dry density of ballast materials. The subgrade layer was compacted in the bottom layer by using OMC% based on the standard -proctor test ($\gamma_t = 14.6$ kN/m³, OMC% = 19).

2.2.4 Parameters of gradation coefficient on the shear strength of sand samples

The experimental results from the 5 × 5 cm and 30 × 30 cm shearing boxes were summarized and analyzed to determine the relationship of τ_{peak} , C_u , C_c , D_{50} and σ . Also, the



(a)



(b)

Fig. 4 Ballasted track system and crushed ballast materials; a) Ballasted track system, b) Particle shape of tested-ballast materials for this study

effect of the B/D_{max} ratio on the shear strength parameter was revealed. The results of the direct shear test of ballast samples on the rigid plate and on the subgrade layers are illustrated.

3 Results and analysis

3.1 Particle size effect on the shear strength of sand based on the 5×5 cm shear box

The 5×5 cm shear box was used in this section to investigate the effect of the particle size on the shear strength of sand. The vertical stress, σ (kPa), of the direct shear test was 1.7, 40.8, 80.2, and 118.7 kPa. According to the experimental result, the relationship of the vertical stress, σ (kPa), the peak shear strength and D_{50} is shown in Fig. 5. The shear strength of sand has the potential to increase when D_{50} increases. The correlation analysis (r_{xy}) can describe the relationship of the maximum shear strength, the vertical stress, and the particle size. In the case that r_{xy} is a positive value, the particle size effect becomes apparent when the sample is compressed by the high vertical stress. The large particle size of samples can provide the high shear strength of the tested sand (Table 2).

The increase of D_{50} provided higher shear strength when the vertical stress is more than 80.2 kPa and the r_{xy} is from 0.8 to 0.9. However, the increase of D_{50} did not affect the increase of the shear strength when the low vertical stress was applied. The relationship of the cohesion (c_{peak} , kPa) and the internal friction angle (ϕ_{peak} , °) based on the Mohr-Coulomb model can be seen in Fig. 6, which was derived from Eqs. (1) and (2). The coefficient of determination (R^2) in terms of cohesion and friction angle was 0.96 and 0.97, respectively, where D_{50} (mm), C_u and C_c were used for predicting the shear strength parameters. The grain size of E-sand varied widely when comparing with other samples thus, it was not considered in this section (Table 3).

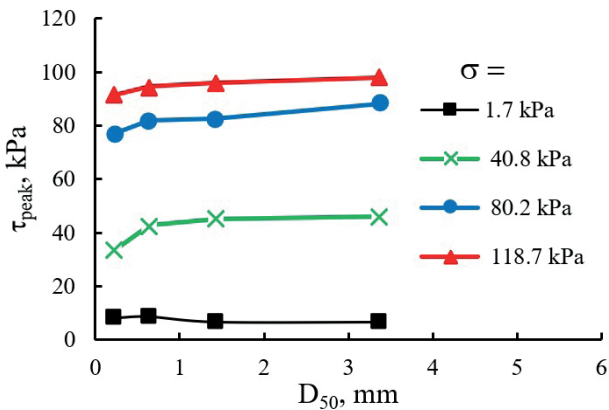


Fig. 5 The variation of shear stress depended on the size of the soil particles and the vertical stress s on the 5×5 -cm box

Table 2 Correlation of D_{50} and peak shear stress

	t_{peak} (kPa)	D_{50} (mm)	r_{xy}
$\sigma = 1.7$ kPa			
A-Sand	6.55	3.375	
B-Sand	6.58	1.425	
C-Sand	8.80	0.638	-0.782
D-Sand	8.25	0.225	
$\sigma = 40.8$ kPa			
A-Sand	30.39	3.375	
B-Sand	45.20	1.425	
C-Sand	42.71	0.638	-0.422
D-Sand	33.41	0.225	
$\sigma = 80.2$ kPa			
A-Sand	88.24	3.375	
B-Sand	42.71	1.425	
C-Sand	82.09	0.638	0.938
D-Sand	76.94	0.225	
$\sigma = 118.7$ kPa			
A-Sand	97.85	3.375	
B-Sand	94.49	1.425	
C-Sand	94.50	0.638	0.895
D-Sand	91.33	0.225	

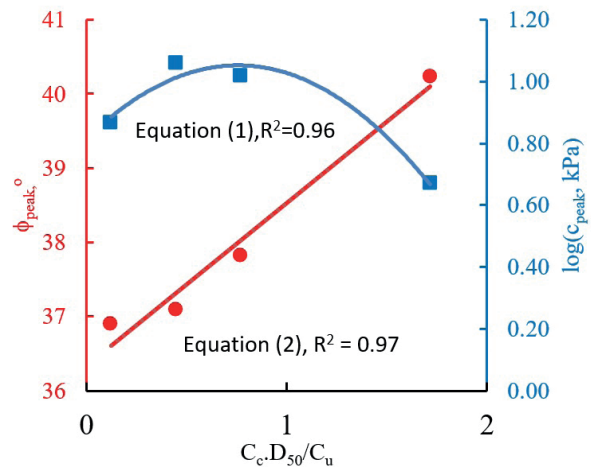


Fig. 6 Relationship of $C_c \cdot D_{50} / C_u$ and shear strength parameters tested by a box sized 5×5 cm

$$c_{peak} (kPa) = 10^\alpha \tag{1}$$

$$\phi_{peak} (^\circ) = 2.194\beta + 36.33 \tag{2}$$

where

$$\alpha = -0.4176\beta^2 + 0.6316\beta + 0.8139$$

$$\beta = C_c D_{50} / C_u$$

According to the regressions from Eqs. (1) and (2), the peak shear strength can be proposed in Eq. (3).

$$\tau_{peak} (kPa) = 10^\alpha + \tan(2.194\beta + 36.33) \tag{3}$$

Table 3 Mohr-Coulomb's parameters of sample groups A, B, C, and D tested by a box sized 5 × 5 cm

Group	c_{peak} (kPa)	ϕ_{peak} °	$C_u \cdot D_{50}/C_u$
A-Sand	4.676	40	1.718
B-Sand	10.508	38	0.768
C-Sand	11.471	37	0.449
D-Sand	7.370	37	0.124

The effect of β , τ_{peak} (kPa), and σ (kPa) can be described as the surface area, as illustrated in Fig. 7, and the variation of peak shear strength of sand depended on both β and the vertical stress on the sample. However, an increase of vertical stress potentially leads to the increase of peak shear strength. The increase of particle size might significantly affect the peak shear strength when the uniformity coefficient (C_u) decreases. This means the higher value of C_u and the lower value of D_{50} are reasons for reduction of the shear strength of sand.

3.2 Effect of the B/D_{max} ratio on shear strength

The effect of the B/D_{max} ratio is generally used to control the particle size of soil samples, and the B/D_{max} ratio ≥ 10 is widely recommended for the sample preparation before testing with the direct shear apparatus. If the particle size of the sample is large, the size of the shear box should be enlarged in the recommended ratio. This ratio determines the reasonable parameters of the shear strength to deeply investigate the details of both soil and box size effects. The experimental result of the direct shear testing with 5 × 5 cm and 30 × 30 cm boxes is discussed in this section, and the particle size of the soil sample is described in Table 4.

Although the two sizes of the shear box were investigated, the three groups of particle sizes could provide the different responses of samples affected by the different B/D_{max} ratio. The parameters obtained resulting from the direct shear tests of sample groups B-Sand, C-Sand, and E-Sand could be determined in terms of the peak cohesion (c_{peak}) and the peak of internal friction angle (ϕ_{peak}) as shown in the previous table. Mohr-Coulomb's parameter was obtained by Fig. 6, and the experimental results of testing on B-Sand, C-Sand, and E-Sand are illustrated in Fig. 8. The results show that the internal friction angle testing with a box size of 30 × 30 cm was higher than those samples testing with a box size of 5 × 5 cm by about ±2 degrees.

According to Fig. 9, the shear strength parameter in terms of cohesion was affected by the B/D_{max} ratio and the cohesion increased when the sample was tested by using the 5 × 5 cm shear box. If the size of the box was changed

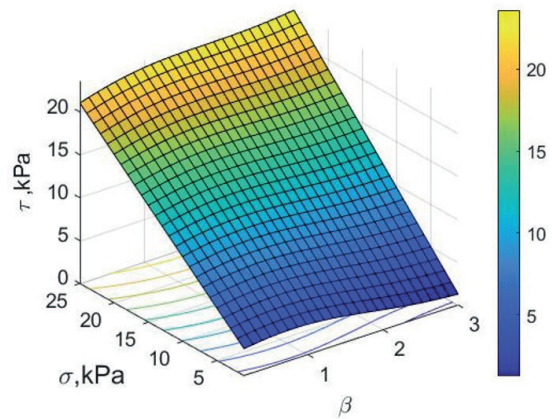


Fig. 7 Relationship of gradation coefficient, τ , and σ tested and formulated using a box sized 5 × 5 cm

Table 4 Mohr-Coulomb's parameters of sample groups B, C, and E tested by boxes sized 5 × 5 cm and 30 × 30 cm

Group	Box sized 5 × 5 cm			Box sized 30 × 30 cm		
	B/D_{max}	c_{peak} (kPa)	ϕ_{peak} °	B/D_{max}	c_{peak} (kPa)	ϕ_{peak} °
B-Sand	25:1	10.51	38	150:1	1.87	38
C-Sand	58.8:1	11.47	37	352.9:1	1.94	37
E-Sand	10.5:1	0	35	63.2:1	0	37

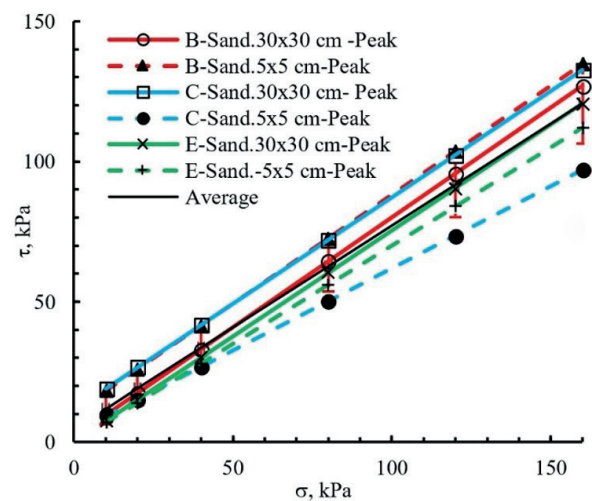


Fig. 8 Relationship of normal and shear stress tested by box sizes of 5 × 5 cm and 30 × 30 cm where $r_{xy} = 1$ for all samples

to 30 × 30 cm, the results showed that the cohesion value is nearly zero, which reflects reasonably on the behavior of the shear strength of the coarse materials when using the larger-sized shearing box. Thus, the B/D_{max} ratio affected the magnitude of the peak shear strength and the cohesion, but not the internal friction angle. The cohesion might be ignored, despite being required for engineering design, when the coarse sand was tested by the 5 × 5 cm shear box in the direct shear test, where the ratio of B/D_{max} might be greater than 10.

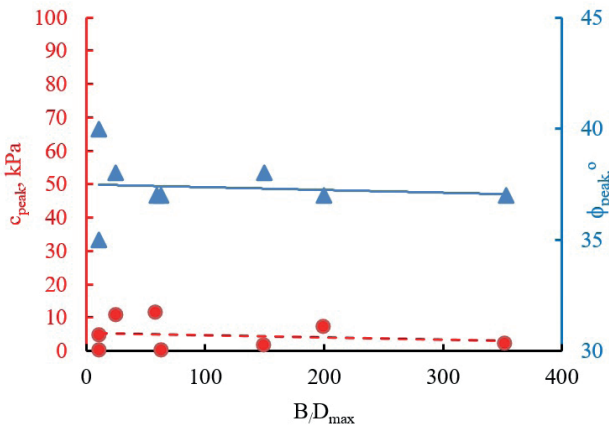


Fig. 9 Effect of shear-box and particle sizes on shear strength parameters

3.3 Effect of the soil bed on the shear strength of ballast materials

The shear strength of ballast materials is to support train loads in horizontal and vertical axes. The horizontal load is also vital when the train reduces speed and is transferred to rails, sleepers, and the ballast layer. If the ballast layer cannot resist the horizontal load, the horizontal displacement can be apparent and cause movement of the rail in the horizontal axis. Also, the poor properties of both ballast and subgrade layer leads to the difference in railway levelling. According to the stress mechanism of the ballast layer, the direct shear test could be used to measure the shear strength of ballast materials. However, the lower layer under the ballast layer is not rigid, which had a potential effect on the magnitude of the shear strength of ballast materials when the shear strength was determined by the direct shear test. In this section, the properties of subgrade materials under the ballast materials were considered in the procedure of the direct shear test. The sample preparation of each sample can be shown in Fig. 10 and described as follows:

B-R was the first group of samples. The ballast materials were placed in the shear box without a subgrade layer, and the base of the shear box was a rigid plate. The total thickness of this sample (H_b) and the height of the shear box were 21.5 cm.

B-S1 was the second group of samples. The tested-ballast material was placed on the top layer in the shear box, and the bottom layer was subgrade materials. The soil subgrade was prepared by the standard proctor test as described in Section 2.2.1. The thicknesses of the tested-ballast layer (H_b) and the subgrade layer (H_s) were 14 cm and 7.5 cm, respectively.

B-S2 was the third group of samples. The top and bottom boxes contained the tested-ballast and subgrade materials, respectively. The thicknesses of the tested-ballast and subgrade layers in the shear box were 6.5 cm, and 15 cm.

During the test, the shear plane for all tests was fixed at 7.5 cm from top of the shear box. The maximum grain size of the tested-ballast is about 30 mm and it was tested with the shear box size of 30×30 cm. The comparison of shear strength parameters is shown in Table 5 and Fig. 11. It reveals that the shear strength of the pure ballast layer on the rigid plate, B-R is lower than the case of B-S1.

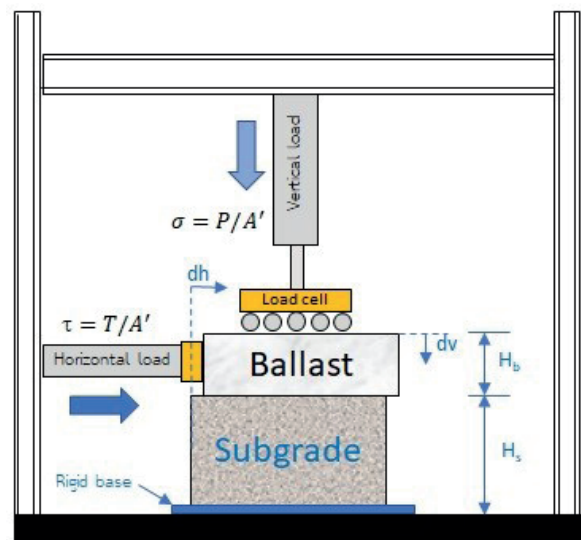


Fig. 10 Ballast and subgrade layers in the shear box

Table 5 Mohr-Coulomb's parameters of B-R, B-S1 and, B-S2

Sample	c_{peak} (kPa)	ϕ_{peak} °
B-R	1.70	45
B-S1	10.88	54.5
B-S2	2.71	52.8

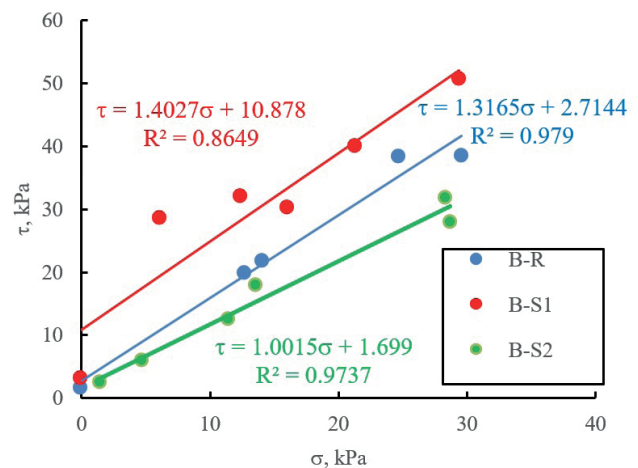


Fig. 11 Effect of the H_b/H_s ratio on Mohr-Coulomb's parameters

However, the internal friction angles of both samples are 52.8° and 54.5° for the cases of B-R and B-S1, respectively, and their internal friction angles were nearly the same angle.

If the ballast layer was installed on the soil bed layer in the shear box, the internal friction angle and the cohesion of the ballast materials decreased when the thickness of the subgrade materials increased. The parameter of the peak-shear strength of the ballast material has potential to be reduced if the ballast layer is supported by a poor and voided subgrade layer. In the case of B-R, the pure ballast layer in the shear box, the development of shear strength depended partially on the movement of ballast materials in all layers. If the vertical displacement increased, the expansion of contacted areas was developed until reaching an equilibrium state. If the vertical displacement became large, and it signified the expansion of the contacted area was developed until reaching the equilibrium state.

However, in the case of a higher vertical displacement that provides lower shear strength, compared to the case of lower vertical displacement, as shown in Fig. 12, the vertical displacement of B-R sample is higher than that of B-S1 sample because the discontinuous contact area was a key for degrading the shear strength of the sample based on the direct shear test. If the bottom layer in the shear box was on rigid materials, the ballast material in the top layer might move upward and the displacement was higher than of the real track.

3.4 Movement and behavior of ballast due to loads

The shear strength of ballast materials can be evaluated by Mohr-Coulomb's envelope. This model is the relationship of vertical stress and shear stress, and it provided higher

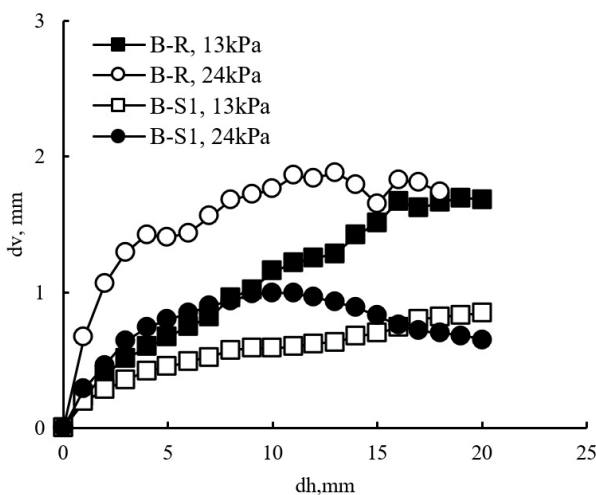


Fig. 12 Effect of the H_b/H_s ratio on vertical and horizontal displacements where $\sigma_1 = 13 \text{ kPa}$ and $\sigma_2 = 24 \text{ kPa}$

cohesion when the ratio of B/D_{\max} was low, and the particle size was large. Therefore, the shear strength parameter of ballast materials in terms of cohesion might appear, although the ballast materials are cohesionless materials. Fig. 13 displays the mechanism of coarse aggregate resisting an inclined load. The direct shear test was used to explore the shear strength and the displacement of ballast materials. The relationship of inclined load was formulated by using the equilibrium equation as in Eqs. (4) and (5) when $+d_v/d_h$ and $\tan \psi = d_v/d_h$.

$$\sum F_{x''} = 0 : T \cos \psi - V \sin \psi = N_r \cdot \sin \phi \tag{4}$$

$$\sum F_{y''} = 0 : T \sin \psi + V \cos \psi = N_r \cdot \cos \phi \tag{5}$$

The relationship of shear strength and vertical stress can be determined as in Eq. (6) when the vertical displacement is a position value.

$$\tau_{\max} = \sigma \frac{(1 + \cot \psi \tan \phi)}{(\cot \psi - \tan \phi)} \tag{6}$$

The variation of shear strength of coarse aggregate under vertical and horizontal loads can be evaluated by changing $\psi(0-20^\circ)$ and $\phi(30-50^\circ)$. In this study, it was found that the increase of ψ induced by the positive vertical displacement leads to an increase of the τ/σ ratio; however, if the ψ angle is smaller than the ϕ angle, the increase of ϕ directly affects the increase of shear strength. So, the effect of ψ angle on the development of shear strength can be ignored when the particle size is very small. The variation of the τ/σ ratio affected by ψ and ϕ angles is illustrated in Fig. 14.

The ratio of ψ/ϕ depended on the particle size of the ballast materials, and the magnitude depended on the ratio of τ/σ . The magnitude of τ/σ is greater than 1 when the internal friction of ballast materials is higher than 45°, as shown in Fig. 15. The peak shear strength might be greater than vertical stress when the internal friction

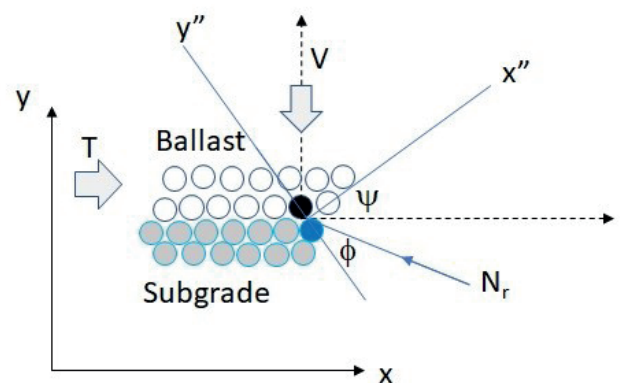


Fig. 13 Sliding of coarse particles

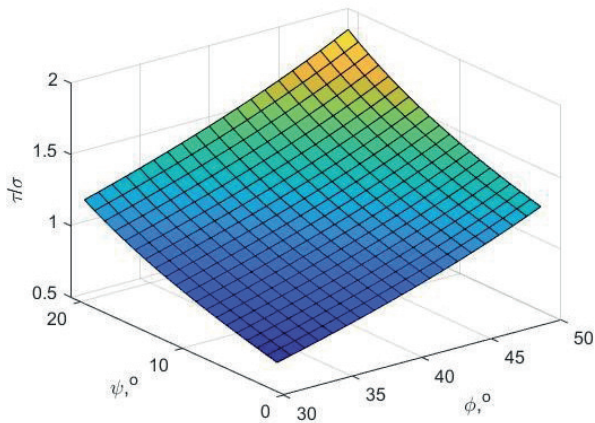


Fig. 14 Relationship of displacement, friction angle, and τ/σ ratio

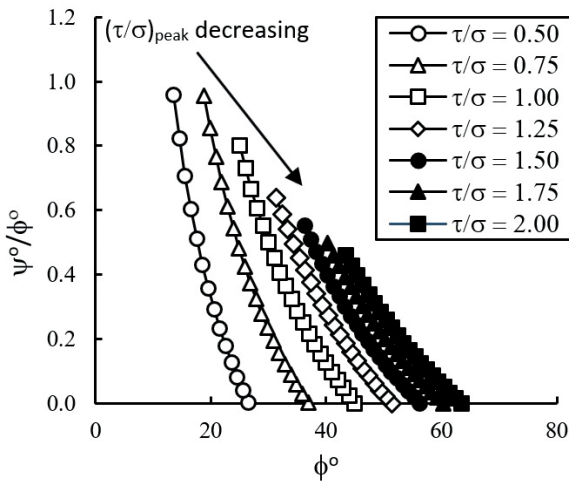


Fig. 15 Variation of friction angle when increasing the ψ/ϕ , and τ/σ ratio

angle is higher than 45° with the lower 0.8 of the ψ/ϕ ratio. Thus, the horizontal displacement has the potential to be reduced when the friction angle of the ballast material is higher than 45° .

The vertical displacement of the ballast layer depends on the relative density of the subgrade layer. If the subgrade layer is ballast materials, the vertical displacement increases because of the properties of voided and unbounded materials. However, if the lower layer is dense without a voiding effect, the vertical displacement is positive, which leads to the increase of the shear strength of ballast materials. This explanation is based on the equilibrium equation. In order to compare, the shear strength parameters obtained by Mohr-Coulomb's concept and, the equilibrium equation, the testing results of B-R and B-S1 samples were compared with both mentioned results in Fig. 16.

In the case of B-R sample, the results show that the shear strength parameter determined by Mohr-Coulomb's envelope can provide the same parameters obtained from the experiments. So, the Mohr-Coulomb's envelope can be

used if subgrade properties are not considered. However, in when considering the property of subgrade materials, the shear strength of ballast material was predicted by Eq. (6), which provided more reliable results than those of the Mohr-Coulomb's concept, especially in the case of B-S1 sample. The shear strength from the experiment is lower than the result predicted from the equilibrium equation. So, the failure line of the ballast layer on the subgrade layer can be formulated when the relationship of H_s/H_b and the modified internal friction angle is equal to Eq. (7).

$$\phi_m(^{\circ}) = \phi_o e^{-0.078H_s/H_b} \quad (7)$$

The yield surface depended on the ratio of the vertical displacement and the horizontal displacement (d_v/d_h) illustrated in Fig. 17 where ϕ_o is the internal friction angle

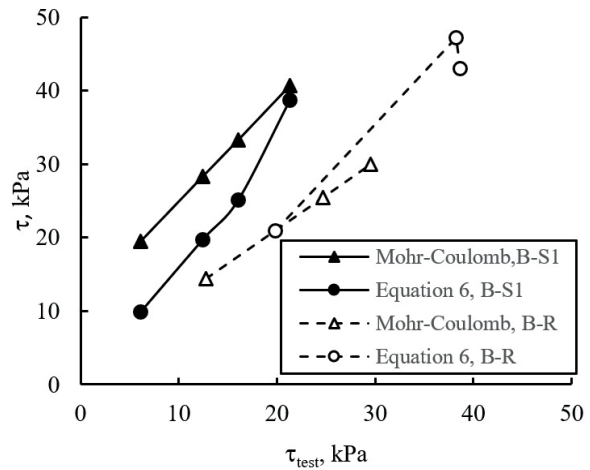


Fig. 16 Comparison between shear strength predicted by models and experiment results

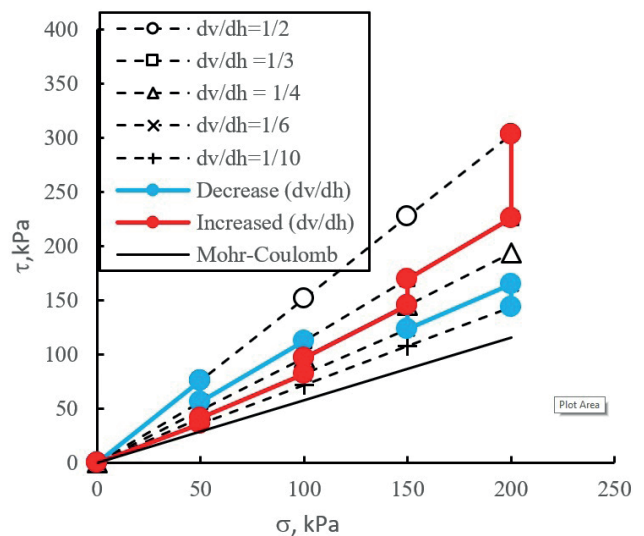


Fig. 17 The failure line of cased $d_v/d_h = 1/2, 1/3, 1/4, 1/6, 1/10$, and Mohr-Coulomb's model of ballast materials, $\phi_m = 30^\circ$ on the subgrade layer

without the effect of the subgrade materials's thickness and ϕ_m is the internal friction angle affected by the subgrade materials's thickness. The ratio of d_v/d_h means the magnitude of dilation of the coarse materials. The failure line might shrink when the ratio of d_v/d_h decreased.

4 Conclusions

This research aimed to investigate the shear strength parameters of ballast and sand materials by using the direct shear test. The main findings of this research can be described as follows:

According to the experimental results performed on the shear box sized 5×5 cm, the shear strength parameters of the Mohr-Coulomb's concept are influenced by the particle size, D_{50} , the uniformity coefficient, C_u , the coefficient of curvature, C_c and the normal stress σ . If the ratio of $C_c D_{50}/C_u$ increases, the internal friction angle increases. However, the cohesion affected from small-shear box of sand sample, decreases when the ratio of $C_c D_{50}/C_u$ is higher than 1. The increase of C_u , the decrease of D_{50} , and the decrease of C_c , that caused the expansion of the void size, led to the lower internal friction angle and shear strength of the sand sample.

The different results obtained from shear boxes sized 5×5 cm and 30×30 cm concerned the shear strength in terms of cohesion, but the internal friction angle is not evidently different. This effect will be apparent, despite the ratio of B/D_{\max} being greater than 25:1, when the particle size is nearly single sizes, and the gradation of soil is poor. The results of well-graded materials tested by 5×5 cm and 30×30 cm shear boxes are the same, and this can be used to determine similar parameters. In the present study, the ratio of B/D_{\max} when is higher than 10:1 results in good agreement for well-graded materials. Thus, higher ratio of

B/D_{\max} is recommended in order to avoid the end boundary effect of the shear box that leads to an overestimated shear strength of the tested materials.

However, the expansion of the shear box might be limited, and this problem can be solved by ignoring the cohesion and reducing the internal friction angle two degrees when the sample is a coarse material and the ratio of B/D_{\max} is nearly 10:1.

The effect of subgrade materials under the ballast layer was not incorporated with the result of the direct shear test, which caused a higher internal friction angle, cohesion, and dilation when the direct shear test was employed to determine the shear strength of ballast materials. Thus, lower shear strength will occur if the stiffness of the subgrade materials is low.

Mohr-Coulomb's envelope can provide the appropriate shear strength parameters when prepared and considering only pure material in the shear box. Besides, the effect of vertical and horizontal displacements might be taken into accounts when determining the shear strength parameter. Without this step, the parameter might be overestimated or underestimated when the stiffness of the subgrade material is low and high, respectively.

The failure line of the ballast materials on the subgrade layer depended on the stiffness of subgrade materials. The decline of the failure line occurs when the ratio of d_v/d_h decrease, and which means the ballast materials move laterally rather than downward, which leads to the decrease of the shear strength of the tested ballast.

Acknowledgement

The authors would like to thank Thipkamnerd W, Nayoung P, Khamwang C who helped some parts of this project in the laboratory.

References

- [1] Gong, H., Song, W., Huang, B., Shu, X., Han, B., Wu, H., Zou, J. "Direct shear properties of railway ballast mixed with tire derived aggregates: Experimental and numerical investigations", *Construction and Building Materials*, 200, pp. 465–473, 2019. <https://doi.org/10.1016/j.conbuildmat.2018.11.284>
- [2] Guo, Y., Wang, J., Markine, V., Jing, G. "Ballast mechanical performance with and without under sleeper pads", *KSCCE Journal of Civil Engineering*, 24(11), pp. 3202–3217, 2020. <https://doi.org/10.1007/s12205-020-2043-5>
- [3] Lam, H. F., Wong, M. T., Yang, Y. B. "A feasibility study on railway ballast damage detection utilizing measured vibration of in situ concrete sleeper", *Engineering Structures*, 45, pp. 284–298, 2012. <https://doi.org/10.1016/j.engstruct.2012.06.022>
- [4] Yang, J., Ishikawa, T., Tokoro, T., Nakamura, T., Kijiyu, I., Okayasu, T. "Effect evaluation of drainage condition and water content on cyclic plastic deformation of aged ballast and its estimation models", *Transportation Geotechnics*, 30, 100606, 2021. <https://doi.org/10.1016/j.trgeo.2021.100606>
- [5] Indraratna, B. "1st Proctor Lecture of ISSMGE: Railroad performance with special reference to ballast and substructure characteristics", *Transportation Geotechnics*, 7, pp. 74–114, 2016. <https://doi.org/10.1016/j.trgeo.2016.05.002>
- [6] Quintanilla, I. D., Combe, G., Emeriault, F., Voivret, C., Ferrellec, J.-F. "X-ray CT analysis of the evolution of ballast grain morphology along a Micro-Deval test: key role of the asperity scale", *Granular Matter*, 21, 30, 2019. <https://doi.org/10.1007/s10035-019-0881-y>

- [7] Medzvieckas, J., Dirgėlienė, N., Skuodis, Š. "Stress-strain states differences in specimens during triaxial compression and direct shear tests", *Procedia Engineering*, 172, pp. 739–745, 2017.
<https://doi.org/10.1016/j.proeng.2017.02.094>
- [8] Mayne, P. W. "A Review of undrained strength in direct simple shear", *Soils and Foundations*, 25(3), pp. 64–72, 1985.
https://doi.org/10.3208/sandf1972.25.3_64
- [9] Hanzawa, H., Nutti, N., Lunne, T., Tang, Y. X., Long, M. "A comparative study between the NGI direct simple shear apparatus and the Mikasa direct shear apparatus", *Soils and Foundations*, 47(1), pp. 47–58, 2007.
<https://doi.org/10.3208/sandf.47.47>
- [10] Stone, K. J. L., Wood, D. M. "Effects of dilatancy and particle size observed in model tests on sand", *Soils and Foundations*, 32(4), pp. 43–57, 1992.
https://doi.org/10.3208/sandf1972.32.4_43
- [11] Liu, S.-H. "Application of in situ direct shear device to shear strength measurement of rockfill materials", *Water Science and Engineering*, 2(3), pp. 48–57, 2009.
<https://doi.org/10.3882/j.issn.1674-2370.2009.03.005>
- [12] Wang, J.-J., Yang, Y., Chai, H.-J. "Strength of a roller compacted rockfill sandstone from in-situ direct shear test", *Soil Mechanics and Foundation Engineering*, 53(1), pp. 30–34, 2016.
<https://doi.org/10.1007/s11204-016-9360-1>
- [13] Xu, W.-J., Xu, Q., Hu, R.-L. "Study on the shear strength of soil–rock mixture by large scale direct shear test", *International Journal of Rock Mechanics and Mining Sciences*, 48(8), pp. 1235–1247, 2011.
<https://doi.org/10.1016/j.ijrmms.2011.09.018>
- [14] Dołyżk-Szypcio, K. "Direct shear test for coarse granular soil", *International Journal of Civil Engineering*, 17, pp. 1871–1878, 2019.
<https://doi.org/10.1007/s40999-019-00417-2>
- [15] Skuodis, Š., Norkus, A., Dirgėlienė, N., Šlečkusienė, A. "Sand shearing peculiarities using direct shear device", *Procedia Engineering*, 57, pp. 1052–1059, 2013.
<https://doi.org/10.1016/j.proeng.2013.04.133>
- [16] Kim, B.-S., Shibuya, S., Park, S.-W., Kato, S. "Effect of opening on the shear behavior of granular materials in direct shear test", *KSCE Journal of Civil Engineering*, 16(7), pp. 1132–1142, 2012.
<https://doi.org/10.1007/s12205-012-1518-4>
- [17] Sanei, M., Faramarzi, L., Fahimifar, A., Goli, S., Mehinrad, A., Rahmati, A. "Shear strength of discontinuities in sedimentary rock masses based on direct shear tests", *International Journal of Rock Mechanics and Mining Sciences*, 75, pp. 119–131, 2015.
<https://doi.org/10.1016/j.ijrmms.2014.11.009>
- [18] Morad, D., Sagy, A., Hatzor, Y. H. "The significance of displacement control mode in direct shear tests of rock joints", *International Journal of Rock Mechanics and Mining Sciences*, 134, 104444, 2020.
<https://doi.org/10.1016/j.ijrmms.2020.104444>
- [19] Li, W., Bai, J., Cheng, J., Peng, S., Liu, H. "Determination of coal–rock interface strength by laboratory direct shear tests under constant normal load", *International Journal of Rock Mechanics and Mining Sciences*, 77, pp. 60–67, 2015.
<https://doi.org/10.1016/j.ijrmms.2015.03.033>
- [20] Härtl, J., Ooi, J. Y. "Experiments and simulations of direct shear tests: porosity, contact friction and bulk friction", *Granular Matter*, 10, pp. 263–271, 2008.
<https://doi.org/10.1007/s10035-008-0085-3>
- [21] Danesh, A., Mirghasemi, A. A., Palassi, M. "Evaluation of particle shape on direct shear mechanical behavior of ballast assembly using discrete element method (DEM)", *Transportation Geotechnics*, 23, 100357, 2020.
<https://doi.org/10.1016/j.trgeo.2020.100357>
- [22] Jia, W., Markine, V., Guo, Y., Jing, G. "Experimental and numerical investigations on the shear behaviour of recycled railway ballast", *Construction and Building Materials*, 217, pp. 310–320, 2019.
<https://doi.org/10.1016/j.conbuildmat.2019.05.020>
- [23] Zhai, M., Xue, L., Chen, H., Xu, C., Cui, Y. "Effects of shear rates on the damaging behaviors of layered rocks subjected to direct shear: Insights from acoustic emission characteristics", *Engineering Fracture Mechanics*, 258, 108046, 2021.
<https://doi.org/10.1016/j.engfracmech.2021.108046>
- [24] Buocz, I., Török, Á., Zhao, J., Rozgonyi-Boissinot, N. "Direct shear strength test on Opalinus Clay, a possible host rock for radioactive waste", In: Lollino, G., Giordan, D., Thuro, K., Carranza-Torres, C., Wu, F., Marinou, P., Delgado, C. (eds.) *Engineering Geology for Society and Territory – Volume 6, Applied Geology for Major Engineering Projects*, Springer, 2014, pp. 901–904. ISBN 978-3-319-09059-7
https://doi.org/10.1007/978-3-319-09060-3_163
- [25] Buocz, I., Rozgonyi-Boissinot, N., Török, Á. "Influence of Discontinuity Inclination on the Shear Strength of Mont Terri Opalinus Claystones", *Periodica Polytechnica Civil Engineering*, 61(3), pp. 447–453, 2017.
<https://doi.org/10.3311/PPci.10017>
- [26] Naghadehi, M. Z. "Laboratory Study of the Shear Behaviour of Natural Rough Rock Joints Infilled by Different Soils", *Periodica Polytechnica Civil Engineering*, 59(3), pp. 413–421, 2015.
<https://doi.org/10.3311/PPci.7928>
- [27] Tejchman, J. "FE-Simulations of a direct wall shear box test", *Soils and Foundations*, 44(4), pp. 67–81, 2004.
https://doi.org/10.3208/sandf.44.4_67
- [28] Hanying, B., Wenping, L., Qiengfeng, D., Qiengfeng, W., Dongdong, Y. "Interaction mechanism of the interface between a deep buried sand and a paleo-weathered rock mass using a high normal stress direct shear apparatus", *International Journal of Mining Science and Technology*, 25(4), pp. 623–628, 2015.
<https://doi.org/10.1016/j.ijmst.2015.05.016>
- [29] Jo, S.-A., Kim, E.-K., Cho, G.-C., Lee, S.-W. "Particle shape and crushing effects on direct shear behavior using DEM", *Soils and Foundations*, 51(4), pp. 701–712, 2011.
<https://doi.org/10.3208/sandf.51.701>
- [30] ASTM "ASTM D 3080 Standard Test Method for Direct Shear Test of Soils Under Consolidated Drained Conditions", ASTM International, Brussels, Belgium, 2012.
<https://doi.org/10.1520/D3080-04>